

# Evaluation of a dual bias dual metal oxide-silicon semiconductor field effect transistor detector as radiation dosimeter

M. Soubra and J. Cygler

Ottawa Regional Cancer Centre, 190 Melrose Avenue, Ottawa K1Y 4K7, Canada

G. Mackay

Thomson & Nielsen Electronics Ltd., 1050 Baxter Road, Ottawa, K2C 3P1, Canada

(Received 15 January 1993; accepted for publication 3 January 1994)

A new type of direct reading semiconductor dosimeter has been investigated as a radiation detector for photon and electron therapy beams of various energies. The operation of this device is based on the measurement of the threshold voltage shift in a custom-built metal oxide-silicon semiconductor field effect transistor (MOSFET). This voltage is a linear function of absorbed dose. The extent of the linearity region is dependent on the voltage controlled operation during irradiation. Operating two MOSFETs at two different biases simultaneously during irradiation will result in sensitivity (V/Gy) reproducibility better than  $\pm 3\%$  over a range in dose of 100 Gy and at a dose per fraction greater than  $20 \times 10^{-2}$  Gy. The modes of operation give this device many advantages, such as continuous monitoring during irradiation, immediate reading, and permanent storage of total dose after irradiation. The availability and ease of use of these MOSFET detectors make them very promising in clinical dosimetry.

Key words: radiation dosimeter, MOSFET

## I. INTRODUCTION

Recently there has been an increased interest<sup>1-3</sup> in the use of metal oxide-silicon semiconductor field effect transistor (MOSFET) as dosimeters for radiotherapy radiation beams. The advantages of MOSFET devices include being a direct reading detector with thin active area ( $< 25 \mu\text{m}$ ) and having a small size. The signal can be permanently stored and is dose rate independent.<sup>2,4</sup> The energy dependence of this detector was investigated for photon radiation<sup>3</sup> and dose enhancement was observed for photon energies below 40 keV where the photoelectric effect is dominant. With adequate filtration added to the MOSFET, uniform response was reported for photon energies above 80 keV.<sup>4</sup> The sensitivity and linearity of MOSFET devices is greatly influenced by the fabrication process and the voltage controlled operation during and after irradiation. MOSFET detectors have been evaluated by other workers for low dose-rate photon irradiation<sup>2</sup> and have been shown to produce a dose uncertainty of 2.5% provided the dose limit does not exceed 10 Gy. The dosimeters used by various workers<sup>1-3</sup> incorporate a single MOSFET as detector in the radiation beam.

In this paper, we report the results of a study performed on a dual bias dual MOSFET, (U.S. Patent No. 4,678,916 and 5,117,113) dosimetry system that is being developed for various clinical photon and electron beam of various energies. This dosimetry system utilizes MOSFET devices that are currently available commercially (Thomas & Nielsen Electronics Ltd., Ottawa, Canada) as dosimeters for nonradiotherapy applications. The dosimetric evaluation will cover detector sensitivity variations as a function of absorbed dose, dose per fraction, bias voltage, and voltage controlled operation during irradiation. In addition comparisons with a single MOSFET detector operating at a single bias have also been performed.

## II. PRINCIPLE OF THE SINGLE MOSFET DETECTOR

### A. MOSFET structure

The basic MOSFET structure is depicted in Fig. 1. The type shown is known as a *P* channel enhancement MOSFET which is built on a negatively doped (*n* type) silicon substrate. Two terminals of the MOSFET called the source (*s*) and the drain (*d*) are situated on top of a positively doped (*p* type) silicon region. The third terminal shown is the gate (*g*). Underneath the gate is an insulating silicon dioxide layer and underneath this oxide layer is the *n* silicon substrate. The region of the substrate immediately below the oxide layer is known as the channel region. When a sufficiently negative  $V_G$  (gate voltage) is applied (with reference to the substrate), a significant number of minority carriers (holes in this case) will be attracted to the oxide-silicon surface from both the bulk of the silicon and the source and drain regions. Once a sufficient number of holes have accumulated there, a conduction channel is formed, allowing an appreciable amount of current to flow between the source and the drain ( $I_{ds}$ ). Figure 2 shows how the magnitude of current varies with gate voltage. Threshold voltage ( $V_{TH}$ ) is defined as the gate voltage needed to attain a predetermined current flow ( $I_{ds}$ ).

### B. The MOSFET as a dosimeter

When a metal-oxide-semiconductor (MOS) device is irradiated, three mechanisms within the silicon dioxide layer predominate:<sup>5</sup> the build-up of trapped charge in the oxide; the increase in the number of interface traps; and the increase in the number of bulk oxide traps.

Electron-hole pairs are generated within the silicon dioxide by the incident ionizing radiation. Electrons, whose mobility in  $\text{SiO}_2$  at room temperature is about 4 orders of magnitude greater than holes,<sup>6</sup> quickly move toward the positively biased contacts. Depending on the applied field

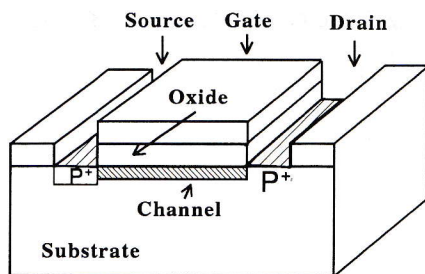


FIG. 1. Schematic cross section of a P channel MOSFET showing the oxide, SiO<sub>2</sub>, the substrate, Si, the source, the gate, and the drain.

and the energy and kind of incident particle, some fraction of electrons and holes will recombine. The holes that escape initial recombination are relatively immobile and remain behind, near their point of generation.

Over a period of about 1 s at room temperature,<sup>7</sup> the holes undergo a stochastic hopping transport through the oxide in response to the applied electric field. When the holes are close (about 5 nm) to the Si-SiO<sub>2</sub> interface, some of them are captured in long-term trapping sites, and cause a negative voltage shift ( $\Delta V_{TH}$ ) that is not sensitive to the silicon surface potential and which can persist for years.

The voltage shift ( $V_{TH}$  before exposure -  $V_{TH}$  after exposure) whose magnitude can be experimentally measured, is proportional to the total quantity of trapped charges which is proportional to the dose. The long-term trapping of holes near the interface is very dependent upon the applied gate voltage and the processing of the SiO<sub>2</sub> layer. Figure 2 shows the negative shift in threshold voltage ( $\Delta V_{TH}$ ) after the MOSFET has been exposed to radiation.

Sensitivity (V/Gy) of the MOSFET can be increased by two methods: (1) A positive gate bias during irradiation will increase hole trapping efficiency by suppressing immediate electron hole recombination in the oxide; and (2) the number of electron-hole pairs generated within the oxide increases with increasing oxide thickness. Experimentally, a clear dependence of radiation sensitivity on oxide thickness has been

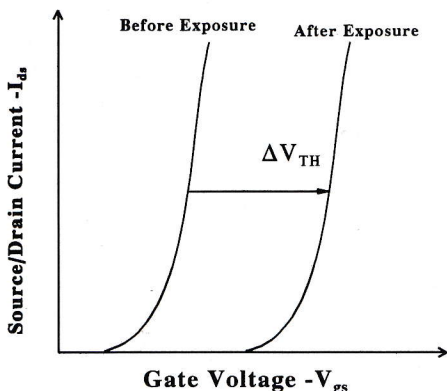


FIG. 2. Typical MOSFET source to drain current,  $I_{ds}$ , vs gate voltage  $V_{gs}$ . The difference in the gate voltages,  $V_{gs}$ , needed to attain a predetermined current flow  $I_{ds}$ , before and after radiation, is equal to the threshold voltage shift ( $\Delta V_{TH}$ ).

observed. For oxides greater in thickness than 20 nm, the threshold voltage  $V_{TH}$ , of oxide-trapped and interface-trap charge, have been found to exhibit a power law dependence on oxide thickness with shifts proportional to  $t_{ox}^n$  where  $t_{ox}$  is the oxide thickness. Values of  $n$  have been reported to vary between 1 and 3.<sup>8</sup> The variation in reported values for  $n$  is primarily due to processing differences such as type of oxide grown (wet vs dry), growth rate, growth ambient pressure, and temperature as well as post oxidation anneal ambient pressure and temperature. The electronics industry traditionally optimizes these process parameters to manufacture radiation "hardened" devices.

Typically commercial MOS transistors have 200 to 800 Å thick gate oxides. To maximize the MOSFET sensitivity to ionizing radiation a relatively thick gate oxide is preferred. However there is a limitation to how thick a gate oxide can be grown. Growth of extremely thick oxide layers ( $>1 \mu\text{m}$ ) requires growth times of greater than 100 h at temperatures of 1000 °C. These oxidation times are not feasible and in addition thick oxide will tend to be highly stressed leading to dislocations at the Si-SiO<sub>2</sub> interface leading to fast surface states and threshold instability.<sup>9</sup>

### III. LIMITATIONS OF THE SINGLE MOSFET DETECTOR

#### A. Temperature

In using a MOSFET as a radiation sensor, care must be taken to distinguish threshold voltage shifts caused by irradiation from those due to changes in temperature. A 1 °C change in ambient temperature can shift  $V_{TH}$  by as much as 4–5 mV for a MOSFET with gate oxide thickness appropriate for use as a sensor.<sup>10</sup> To overcome the effects of temperature changes on the sensor, the dual bias dual MOSFET detector can be used and is described in more details later.

#### B. Linearity

The response of the single MOSFET detector ( $\Delta V_{TH}$ ) as a function of accumulated dose will exhibit a nonlinear region at high dose levels. The main reason for this phenomena is the accumulation of the radiation generated positive charge (holes) in the oxide traps which effectively reduces the magnitude of the electric field produced by the positive gate bias between the positive charge region and the gate. The reduced local fields in the oxide lead to enhanced electron/trapped-hole recombination and thus diminish the voltage shift measured.<sup>11</sup> As will be shown, the nonlinear response at high dose levels can be reduced through the use of the dual bias dual MOSFET detector.

### IV. PRINCIPLES OF THE DUAL BIAS DUAL MOSFET DETECTOR

#### A. Device design and operation

The dual bias dual MOSFET detector consists of two identical MOSFETS fabricated on the same silicon chip. These two identical MOSFETS operate at two different positive gate bias and are irradiated simultaneously by ionizing radiation when used as dosimeters. The basic structure and

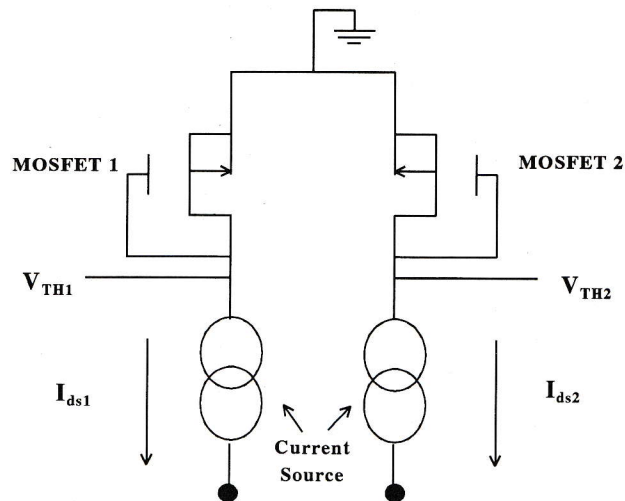


FIG. 3. Readout circuitry for the threshold voltages  $V_{TH1}$  and  $V_{TH2}$  of each MOSFET in the sensor pair. 100  $\mu\text{A}$  current,  $I_{ds1}$  and  $I_{ds2}$ , between the source and drain are maintained during readout.

principle of operation of each of the MOSFETs in the dual dosimeter is similar to that of the single MOSFET described in the previous section. Upon irradiation each of the sensors will produce a threshold voltage shift whose magnitude increases when the positive gate bias is raised. The measured difference between the threshold voltage shifts of the two sensors ( $\Delta V_{TH1} - \Delta V_{TH2}$ ), is representative of the absorbed dose and the magnitude of this difference per unit dose (i.e., sensitivity) will be shown to be constant and independent of the total absorbed dose studied in this work.

### B. Readout circuitry

To read the threshold voltage of each MOSFET in the detector the circuit configuration shown in Fig. 3 has been used. In essence a 100  $\mu\text{A}$  current source is connected to the source of the MOSFET while the gate is tied to the drain. The potential difference between the gate and substrate,  $V_{gs}$ , is then measured before and after irradiation using a conventional 4-1/2 digit volt meter. In this approach the "threshold voltage"  $V_{TH}$  is defined to be the value of gate voltage  $V_{gs}$  which must be applied to maintain  $I_{ds}$  at 100  $\mu\text{A}$ . Typically the virgin MOSFET dosimeters have initial threshold voltages between  $-4.5$  to  $-5$  V. This read circuit was used to measure  $V_{TH}$  of both the single and dual configuration MOSFET dosimeter.

## V. EXPERIMENTAL MEASUREMENTS

### A. Setup

The experimental configuration consisted of a test head (see Fig. 4) that can accommodate MOSFET devices, a control box that operates a dc voltage power supply and a 4-1/2 digit volt meter. During irradiation the single MOSFET dosimeters were biased at various voltages ranging from 0–40 V while the dual MOSFET dosimeter had one sensor biased at 3 V and the second sensor was biased at 5 to 30 V.

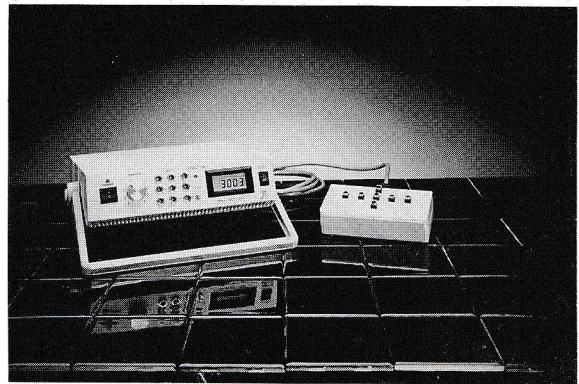


FIG. 4. Test head that accommodates MOSFET devices and a control box that operates the dc voltage power supply and the 4-1/2 digital voltmeter.

To switch the MOS devices from BIAS mode to TEST mode the test head was connected to a control box situated beside the control console via a 30 m cable. After irradiation a mechanical switch was used to connect the MOSFET(S) from the BIAS circuit to the TEST circuit. An adjustable power supply was connected to input jacks of the control box to provide BIAS to the MOSFET(S) thus increasing their sensitivity to ionizing radiation. When the control box placed the MOSFET device(s) into TEST mode, the 4-1/2 digital volt meter was used to read the individual threshold voltages.

### B. Irradiation setup

During irradiation with clinical electron beams the test head was placed at depth of maximum dose in a full scatter polystyrene phantom with the sensor center positioned along the beam axis. Electron beams of 6, 9, 13, 17, and 20 MeV energies produced by clinical linear accelerators (Siemens Mevatron KD2 and A.E.C.L. Therac 20) were used for the detector irradiation. The absorbed dose quoted in this work is for a homogenous water phantom in which absolute dose calibrations were made using TG21 protocol at the appropriate depth. The accelerator output was checked for every measurement with a Farmer type ionization chamber that was placed into a machined insert in the polystyrene phantom and irradiation reproducibility better than 0.3% was obtained. A  $10 \times 10$  cm<sup>2</sup> field size was used with the phantom surface at 100 cm from the source. Another set of similar measurements were performed in a Co-60 beam with the MOSFET detectors positioned at 5 cm depth in a polystyrene phantom with its surface at 80 cm from the source. A  $10 \times 10$  cm<sup>2</sup> field opening was set. Most of the MOSFETs irradiated in this work were operated at different bias voltages ( $V_{gs}$ ). The maximum absorbed dose reached for some of these detectors was in excess of 300 Gy and repeated measurements under the same setup and bias but with a different MOSFET has similar results within  $\pm 2\%$  reproducibility.

Throughout the irradiation experiments the room temperature was checked and verified to be constant within  $\pm 0.1$  °C.

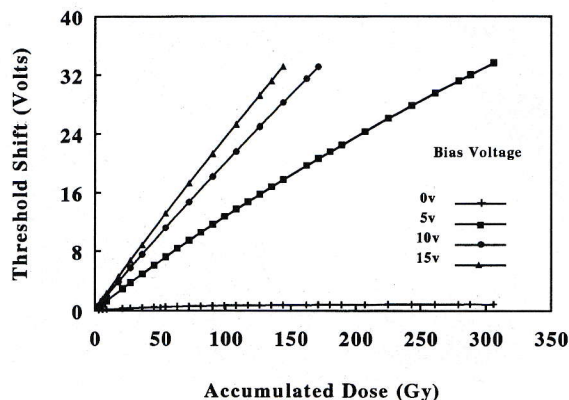


FIG. 5. Threshold voltage shift,  $\Delta V_{TH}$ , of a single MOSFET as a function of accumulated dose at different gate biases,  $V_{gs}$ , (0, 5, 10, and 15 V) from a 13 MeV electron beam.

## VI. RESULTS AND DISCUSSION

### A. Single MOSFET detector

The threshold voltage shift,  $\Delta V_{TH}$ , as a function of increased absorbed dose is shown in Fig. 5 for unbiased and 5, 10, and 15 V biased MOSFETs exposed to a 13 MeV electron beam. After irradiation to 315 Gy the shift in  $V_{TH}$  was about 0.9 and 34 V for the unbiased and 5 V biased sensor, respectively. In case of the 15 V biased MOSFETs the  $V_{TH}$  shift has reached about 33 V after an exposure to lower dose of 171 Gy. For all the energies and qualities of radiation studied in this work, the linearity of sensor response vs dose improves with a higher bias voltage. However, the lower sensitivity associated with a lower gate bias enables the MOSFET to be radiated to higher accumulated dose. In this work the maximum  $V_{TH}$  shift that could be read was limited to 50 V since when operating above this level caused a decrease in the detector circuit stability.

Figure 6 shows the variation of the MOSFET dosimeter sensitivity ( $\Delta V_{TH}$ )/Gy as function of the positive gate bias  $V_{gs}$  for a 9 MeV electron beam. Increasing  $V_{gs}$  results in

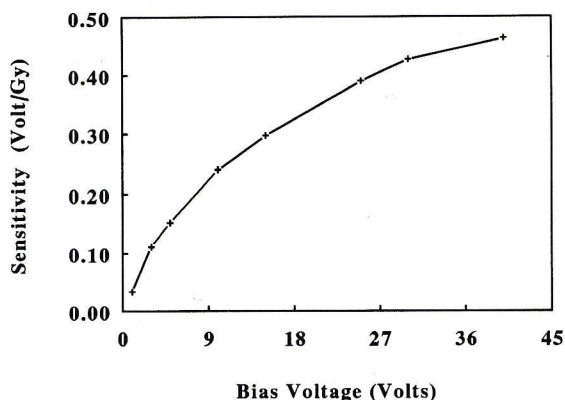


FIG. 6. Sensitivity, V/Gy, as a function of the MOSFET gate bias,  $V_{gs}$ , for 9 MeV electron beam.

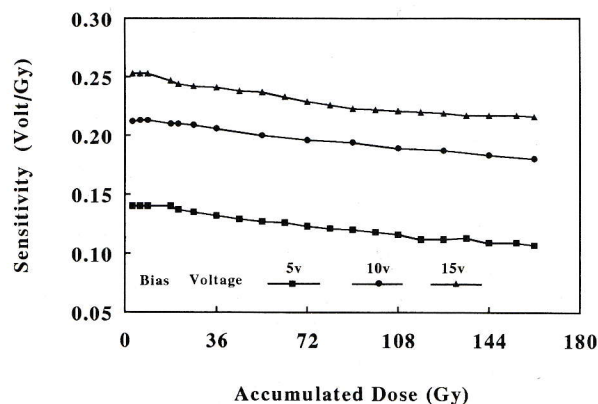


FIG. 7. Single MOSFET device. Sensitivity, V/Gy, as a function of accumulated dose at different gate biases,  $V_{gs}$  (5, 10, and 15 V) from a 13 MeV electron beam.

increased device sensitivity until saturation occurs. This happens when most of the holes created by incident radiation escape recombination and are captured by the oxide and interface traps. Any further increase in the sensor sensitivity can only be achieved by increasing the oxide thickness as mentioned before.

Similar results were seen for the different electron energies investigated.

Figure 7 illustrates the decrease in MOSFET response observed as a function of accumulated radiation dose from a 13 MeV electron beam for 5, 10, and 15 V bias ( $V_{gs}$ ). The data show a continuous decrease in sensitivity with increased dose and the effect is more apparent for the sensors operating at lower bias voltage during irradiation. After exposure to 46 Gy a 23% drop in sensitivity was observed for the MOSFET biased at 5 V, while for the 10 and 15 V biased detectors the sensitivity decrease was only 16%. For the other energies and qualities of radiation studied, the percentage drop in sensitivity with increased dose was within the same level as above for similar biases and irradiation conditions.

Since the sensitivity changes with increased cumulative dose are reproducible characteristics of the MOSFET, correction could be applied if the detector response as a function of dose is known *a priori*. This means that similar data to Fig. 7 have to be generated for the appropriate bias voltage. However, the dual bias dual MOSFET technique discussed below eliminates the need to generate this data and reduces sensitivity changes with increased dose.

### B. Dual bias dual MOSFET technique advantages

#### a. Linearity

Figure 7 shows that the sensitivity for individual MOSFET biased at 5, 10, and 15 V are parallel indicating that the magnitude of the sensitivity difference of two dissimilar biased MOSFETs is constant over the absorbed dose investigated. This is due to the fact that for two dissimilar biased MOSFETs the difference in the number of trapped holes near the Si-SiO<sub>2</sub> interface remains constant over the range studied in this work. To verify this performance a series of

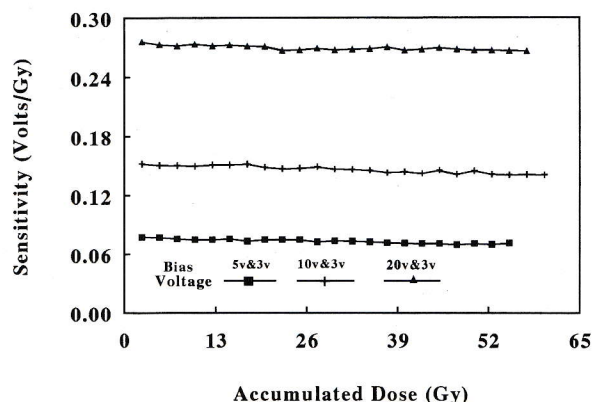


FIG. 8. Dual bias dual MOSFET device. Sensitivity  $(\Delta V_{TH1} - \Delta V_{TH2})/\text{dose}$  as a function of accumulated dose for Co-60 beam, at different gate biases.

measurements were made for a Co-60 beam with a sensor containing two identical MOSFETs with one maintained at a constant bias of 3 V while the other was biased to a different  $V_{gs}$ . The data were collected in steps of 2.50 Gy exposure with one of the MOSFETs biased to one of these values: 5, 10, 20, and 30 V. Figure 8 shows the effects of these two bias techniques on the response of the sensor. An improvement in the linearity of the sensitivity  $[(\Delta V_{TH1} - \Delta V_{TH2})/\text{unit dose}]$  as a function of accumulated dose has been observed and this effect is most apparent when the difference between the bias voltages of the two MOSFETs is greatest. With one of the MOSFETs biased to 20 V, a decrease in sensitivity of only 2% was obtained after a dose of 70 Gy. This is an advance over the single bias voltage method where the measured drop in sensitivity under the same exposure conditions was 30% and 10% when a single MOSFET was biased to 3 and 20 V, respectively. In case when one of the MOSFETs was biased to 30 V the total dose delivered was 100 Gy and the sensitivity drop over the range was less than 1.5%.

## 2. Sensor reproducibility

The precision of the MOSFET response has been evaluated with the detector operating in the two biases (20 and 3 V) technique. Multiple fractions from Co-60 beam irradiation were performed and the detector reproducibility was studied as a function of dose per fraction. Table I lists the dose per fraction, the number of fractions and the mean of  $(\Delta V_{TH1} - \Delta V_{TH2})$  with its associated maximum deviation as

TABLE I. Precision of MOSFET response.

Dose/fraction (Gy)	# of fractions	$(\Delta V_{TH1} - \Delta V_{TH2})$ Volts $\times 10^{-3} \pm \% \epsilon^a$
$3.5 \times 10^{-2}$	27	$10.6 \pm 9.4$
$7.3 \times 10^{-2}$	21	$21.5 \pm 7.0$
$20.7 \times 10^{-2}$	16	$58.0 \pm 3.4$
$59.1 \times 10^{-2}$	18	$164.5 \pm 1.5$
2.50 <sup>b</sup>	22	$675.0 \pm 1.2$

<sup>a</sup> $\pm$  maximum deviation from the mean.

<sup>b</sup>Reading is obtained with a different sensor.

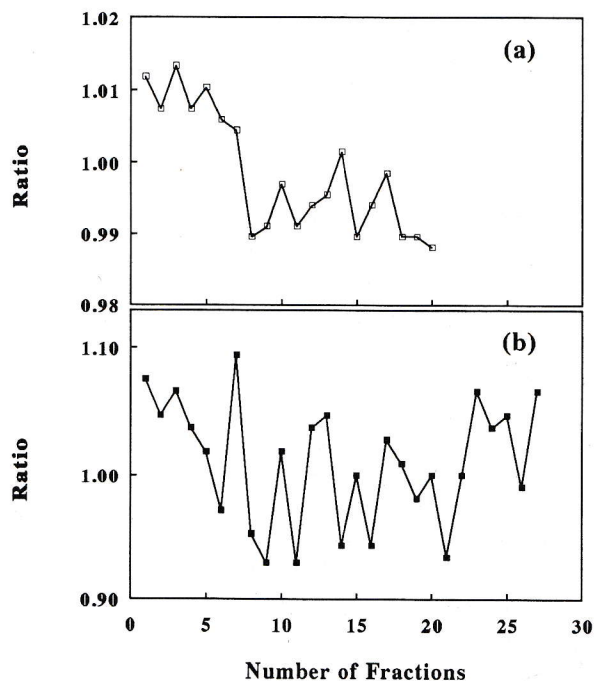


FIG. 9. The variation of the dual MOSFET dual bias device (20 and 3 V) response from the mean value as a function of number of fractions for (a) 2.5 Gy/fraction and (b)  $3.5 \times 10^{-2}$  Gy/fraction.

a percentage of the mean. In addition Figs. 9(a) and 9(b) illustrate the variation in the device response from the mean value for 2.5 and  $3.5 \times 10^{-2}$  Gy/fraction, respectively, as a function of number of fractions. As Table I indicates, at the lowest dose per fraction of  $3.5 \times 10^{-2}$  Gy the MOSFET response was reproducible within  $\pm 9.4\%$  ( $\pm 1$  mV). As the dose per fraction increases an improvement in the sensor reproducibility is obtained reaching a value within  $\pm 1.2\%$  ( $\pm 8$  mV) for 2.5 Gy/fraction.

## 3. Sensor stability

Two identical MOSFETs in the same circuit operating at 6 and 3 V bias, respectively, were irradiated to a dose of 6 Gy from a Co-60 beam and the value of  $(\Delta V_{TH1} - \Delta V_{TH2})$  was monitored over a period of 35 days post irradiation while the bias voltages were applied. A continuous increase up to 4% in the sensor reading at the end of the monitoring period was measured. This can be attributed to the time dependent delayed buildup of the positively charged interface traps<sup>12</sup> that cause the negative threshold voltage to decrease continually. Consequently, an increase in the threshold voltage shift should occur and this has been observed above.

## 4. Temperature effects

Since the dual bias dual MOSFETs dosimeter consists of a matched pair of MOSFET transistors fabricated on the same silicon substrate and they are operated at low power levels, the response to temperature of each individual MOSFET is identical. Consequently, the incorporation of the dual MOSFETs in the dosimeter will render minimal temperature effects.

The difference in threshold voltage shifts ( $\Delta V_{TH1} - \Delta V_{TH2}$ ) was monitored as a function of temperature (0–80 °C) for a detector previously irradiated to 10 Gy with a resultant temperature coefficient of 0 to 0.015 mV/°C.

## VII. CLINICAL RELEVANCE

Currently in many radiotherapy departments thermoluminescence dosimeters (TLDs) and diode detectors are used extensively for absorbed dose verification during patient treatments. TLDs require a relatively long preparation time before and after irradiation in order to obtain acceptable readout dose accuracy. Diodes are on-line dosimeters and operate in continuous charge integration mode which necessitates the use of cables to measure the signal. This may be cumbersome in clinical setups where many diodes are used simultaneously on the patient such as in whole body treatments. Both of these dosimeters lose the dose history after readout. In comparison, the MOSFET dosimeter has the ability of storing the total dose after irradiation and its response is reproducible to an uncertainty of about  $\pm 3\%$  at doses greater than  $20 \times 10^{-2}$  Gy if the dual bias-two MOSFETs technique is applied. This uncertainty limit is comparable with TLDs dose response, however, at lower doses the MOSFET suffers reduced precision (see Table I). Due to the low power needs of the MOSFET a small dc battery can be incorporated with the miniature circuitry that can be connected to the sensor during irradiation thus providing the adequate bias(es). This system can be made to have minimum interference by the radiation fields used during treatment. In development is a system that will have the capability of using the dual bias-two MOSFET technique. This device can be placed on patients without the need of cables and the voltage shift which is indicative of the absorbed dose can be measured with a voltmeter after the completion of treatment.

## VIII. CONCLUSIONS

A new type of dosimeter, MOSFET, was evaluated as a radiation detector for clinical electron and photon beams. The operation of this device is based on measurement of the threshold voltage shift which is proportional to the total absorbed dose. Depending on the technique of biasing this sensor during irradiation, a linear response as function of dose

can be obtained. For two MOSFETs biased differently and exposed simultaneously to ionizing radiation, the sensitivity reproducibility is better than 3% over an accumulated dose range of 100 Gy provided the dose per fraction is greater than  $20 \times 10^{-2}$  Gy. Although this reproducibility is comparable with the one obtained for the TLDs, the strong advantages of MOSFETs lie in the instant readout, portability, and permanent storage of the dose. Its small size, requirement of low power, and simple readout circuit make this dosimeter very promising for clinical applications.

## ACKNOWLEDGMENTS

The authors wish to thank the following for their useful discussion and comments for this work. I. Thomson of Thomson & Nielson Electronics LTD, Ottawa, Canada, D. W. Rogers of Ionising Radiation Standards, NRC, Ottawa, Canada, J. Dubeau of Thomson & Nielson Electronics, LTD, Ottawa, Canada, and N. G. Tarr, Department of Electronics, Carleton University, Ottawa, Canada.

- <sup>1</sup>R. C. Hughes, D. Huffman, J. V. Snelling, J. E. Zipperian, A. J. Ricco, and A. Kelsey, "Miniature Radiation Dosimeter for In-Vivo Radiation Measurements," *Int. J. Radiat. Oncol. Biol. Phys.* **14**, 963–967 (1988).
- <sup>2</sup>D. J. Gladstone and L. M. Chin, "Automated Data Collection and Analysis System for MOSFET Radiation Detectors," *Med. Phys.* **18**, 542–548 (1991).
- <sup>3</sup>C. Sharland and D. Smith, "Application of MOS Dosimeters," *IEEE Symposium on Modern Methods of Detecting and Measuring Ionizing Radiation*, London, U.K. (1992).
- <sup>4</sup>M. H. Reece and I. Thomson, "Semiconductor MOSFET Dosimetry," *Proceedings of Health Physics Society Annual Meeting* (1988).
- <sup>5</sup>I. Thomson, R. E. Thomas, and L. P. Berndt, "Radiation Dosimetry with MOS Sensor," *Radiation Protection Dosimetry* **6**, 121–124 (1984).
- <sup>6</sup>R. C. Hughes, "Charge-Carrier Transport Phenomena in Amorphous SiO<sub>2</sub>: Direct Measurement of the Drift Mobility and Lifetime," *Phys. Rev. Lett.* **30**, 1333 (1973).
- <sup>7</sup>R. C. Hughes, "Time Resolved Hole Transport in a SiO<sub>2</sub>," *Phys. Rev. B* **15**, 2012 (1977).
- <sup>8</sup>P. V. Dressendorfer, in *Ionizing Radiation Effects in MOS Devices and Circuits*, Chap. 6, edited by T. P. Ma and P. V. Dressendorfer, 1st ed. (Wiley, New York, 1989).
- <sup>9</sup>*VLSI Technology*, edited by S. M. Sze (McGraw-Hill, New York, 1983).
- <sup>10</sup>I. Thomson, G. Mackay, and N. G. Tarr, "Gamma Ray Dosimetry Using a MOSFET-Based Sensor Chip," *Proceedings of the Canadian Conference on Very Large Scale Integration* (1990).
- <sup>11</sup>H. E. Boesh, Jr. and J. M. McGarrity, "Charge Yield and Dose Effects in Mos Capacitors at 80 K," *IEEE Trans. Nucl. Sci.* **NS-33**, 1520 (1976).
- <sup>12</sup>P. S. Winokur, in Ref. 8.